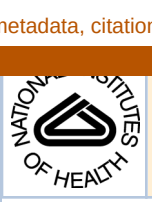

Published in final edited form as:
Biochemistry. 2012 January 17; 51(2): 695–705. doi:10.1021/bi201034z.

Characterization of the redox activity and disulfide bond formation in Apurinic/apyrimidinic endonuclease

Meihua Luo[‡], **Jun Zhang**[‖], **Hongzhen He**[§], **Dian Su**[⊥], **Qiujia Chen**[§], **Michael L. Gross**[‖], **Mark R. Kelley**[*,‡], and **Millie M. Georgiadis**[*,§,⊥]

[‡]Section of Pediatric Hematology and Oncology, Department of Pediatrics, Washington University in St. Louis, St. Louis, Missouri

[§]Department of Biochemistry and Molecular Biology, Indiana University School of Medicine, Washington University in St. Louis, St. Louis, Missouri

[‖]Department of Chemistry, Washington University in St. Louis, St. Louis, Missouri

[⊥]Department of Chemistry and Chemical Biology, Purdue School of Science, Indiana University-Purdue University Indianapolis, Indianapolis, Indiana 46202

Abstract

Apurinic/apyrmidinic endonuclease (APE1) is an unusual nuclear redox factor in which the redox-active cysteines identified to date, C65 and C93, are surface inaccessible residues whose activities may be influenced by partial unfolding of APE1. To assess the role of the remaining five cysteines in APE1's redox activity, double cysteine mutants were analyzed excluding C65A, which is redox-inactive as a single mutant. C93A/C99A APE1 was found to be redox-inactive whereas other double cysteine mutants retained the same redox activity as that observed for C93A APE1. To determine whether these three cysteines, C65, C93, and C99, were sufficient for redox activity, all other cysteines were substituted with alanine, and this protein was shown to be fully redox active. Mutants with impaired redox activity failed to stimulate cell proliferation, establishing an important role for APE1's redox activity in cell growth. Disulfide bond formation upon oxidation of APE1 was analyzed by proteolysis of the protein followed by mass spectrometry analysis. Within 5 min. of exposure to hydrogen peroxide, a single disulfide bond formed between C65 and C138 followed by the formation of three additional disulfide bonds within 15 min.; ten total disulfide bonds formed within one hour. A single mixed-disulfide bond involving C99 of APE1 was observed for the reaction of oxidized APE1 with TRX. Disulfide-bonded species of APE1 or APE1/TRX were further characterized by size exclusion chromatography and found to form large complexes. Taken together, our data suggest that APE1 is a unique redox factor with properties distinct from those of other redox factors.

Cells are continually subjected to reactive oxygen species resulting from normal metabolic processes as well as from exogenous sources and have in place mechanisms to repair damage to cellular components (reviewed in (1)). Oxidative damage to proteins, which can lead to loss of function through the formation of disulfide bonds, is repaired by general redox factors such as thioredoxin or glutaredoxin or, in the case of nuclear proteins, by the

[*]To whom correspondence should be addressed: M.M.G.: telephone, (317) 278-8486; fax, (317) 274-4686; *mgeorgia@iupui.edu* or M. R. K.: telephone, (317) 274-2755; fax, (317) 274-5378;, mkelley@iupui.edu..

Supporting Information Available

The supporting information contains CD spectra for wild-type APE1, APE1 C65/C93 and APE1 C65/C99. This material is available free of charge via the Internet at http://pubs.acs.org.

multifunctional DNA repair and redox factor apurinic/apyrmidinic endonuclease (APE1) or Ref-1 (2).

APE1 is a multifunctional protein that serves as an essential base excision repair protein and, as a nuclear redox factor, regulates the activity of a number of important transcription factors (reviewed in (2)). Its role in regulating transcriptional activity through a redox mechanism was first established for AP-1 (c-Jun/c-Fos)(3, 4) and later shown for a number of other transcription factors including NF-κB(5-7), HIF-1α(8), and p53(9). The idea that AP-1 may be under redox regulation in the cell came in part from the observation that the oncogene v-Jun with a Cys to Ser substitution in the DNA-binding domain of the protein was no longer under cellular regulation. This finding suggested that redox regulation of AP-1 might be mediated by a thiol-exchange mechanism. Of the seven Cys residues present in APE1, a single Cys-to-Ala substitution, C65A, resulted in the loss of APE1's redox activity (10). In this same study, oxidized C93A APE1 was shown to retain redox activity. We found in previous studies that none of the oxidized APE1 mutants retained redox activity, but the reduced C93A APE1 was significantly less redox active than wild-type APE1, while C65A APE1 was completely redox inactive (11).

We next examined the conservation of Cys residues in vertebrates and discovered that Cys 65 is conserved only in mammals; the residue in zebrafish APE equivalent to Cys 65 is Thr 58 (12). Through substitution of Thr 58 with a Cys residue (T58C), zebrafish APE gains redox function both in EMSA redox assays and cell-based transactivation assays; wild-type zebrafish APE1 retains repair activity but lacks redox activity (11). Additionally, redox-active T58C zebrafish APE1 was inhibited by an APE1 redox specific small molecule (11). Of the seven cysteines in human APE1, all except Cys 65 and Cys 138 are conserved in zebrafish APE, but no disulfide bonds are observed in the crystal structures of zebrafish APE (11) or human APE1 (11, 13-15). In fact, none of the cysteines are positioned appropriately or close enough to form intramolecular disulfide bonds in either protein.

The first question we sought to answer in the present study is what role, if any, the remaining five Cys residues (other than C65 and C93) play in APE1's redox activity. We next examined the role of APE1's redox activity in cell growth by characterizing growth for cells expressing redox-active vs. redox-impaired APE1. As a redox factor, APE1 is necessarily oxidized and subsequently reduced by a cellular redox factor, such as thioredoxin. Therefore, we examined disulfide bond formation in oxidized APE alone or reacted with thioredoxin. Finally, we further characterized disulfide-bonded APE1 and APE1/TRX by size exclusion gel chromatography.

Experimental Procedures

Preparation of proteins and mutants

Mutations resulting in the following substitutions C65A, C93A/C99A, C93A/C138A, C93A/C208A, C93A/C296A, C93A/C310A were introduced in hAPE1 encoded within a pGEX-3X vector through site-directed mutagenesis by using the Stratagene Quikchange kit and confirmed by DNA sequencing. GST-APE1 proteins were expressed and purified as previously described(11).

APE1 mutants including only specific Cys residues with all others as Ala, C65, C65/C93, C65/C99, C93/C99, C65/C93/C99 APE1 were introduced through site-directed mutagenesis into an N-terminal hexa-His-SUMO-fusion (Invitrogen; Rockville, MD) by using the Stratagene Quikchange kit and confirmed by DNA sequencing. These proteins were expressed and purified, as previously reported for wild-type APE1, by using Ni-NTA

affinity chromatography, on-column Ulp1 cleavage, followed by SP-Sepharose ion-exchange chromatographic separation(16).

The thioredoxin mutant including only C32 (TRXC32) with Cys 35 mutated to Ser and all other Cys residues mutated to Ala was created by using site-directed mutagenesis of a plasmid encoding TRX cloned into pET15b and confirmed by DNA sequencing. TRXC32 was expressed and purified as previously described for thioredoxin(16).

For transactivation assays, mutations were introduced through site-directed mutagenesis in the pcDNA-wtAPE1 vector by using the Stratagene Quikchange kit and confirmed by DNA sequencing. The following mutants were generated: C65A, C93A, C99A, C138A, C208A, C93A/C99A, C93A/C99A/C138A, and C93A/C99A/C138A/C208.

Electrophoretic mobility shift assay (EMSA)

EMSAs were performed as described (12) with the following modifications; 0.3 mM purified APE1 and its mutant proteins were reduced with 1.0 mM DTT for 10 min and diluted to a final concentration of 0.006 mM with 0.02 mM DTT in PBS. Reduced APE1 (2 μL) or its mutant proteins were added to EMSA reaction buffer (10 mM Tris (pH 7.5), 50 mM NaCl, 1 mM $MgCl_2$, 1 mM EDTA, 5% [vol/vol] glycerol) with 2 μL 0.007 mM protein mixture (1:1) of purified truncated c-Jun and c-Fos proteins containing DNA-binding domain and leucine zipper region in total volume 18 μL and incubated for 30 min. at room temperature. The EMSA assay was performed as previously described (12, 16, 17).

Transactivation assays

Skov-3X cells containing the NFκB- Luc gene reporter were cotransfected with a control pcDNA empty vector plasmid, pcDNA-wtAPE1 or pcDNA-APE1 mutants and a *Renilla* luciferase control reporter vector, pRL-CMV (Promega Corp., Madison, WI), in a 1:10 ratio using lipofectamine TM 2000. After 30 h transfection, cells were lysed and the *Firefly* and *Renilla* luciferase activities were assayed using the Dual Luciferase System (Promega Corp., Madison, WI) with Renilla luciferase activity for normalization in a 96-well microtiter plate luminometer (Thermolabs systems, Franklin, MA). All of the transfection experiments were performed in triplicate and repeated at least three times as independent experiments.

Enzyme kinetic assays

AP endonuclease activity for recombinant proteins APE1 and APE1C65/C93/C99 was measured in a fluorescent-based kinetic assay by using a duplex DNA substrate containing a tetrahydrofuran abasic site mimic as the substrate. The assay employs fluorescein and dabcyl as a fluor-quench pair in the following oligonucleotides (5′-6- FAM- GCC GAC FGA GGA CGT ACG CG -3′ and 5′- CGC GTA CGT CCT CTG TCG GC -Q-3′) from Eurogentec Ltd (San Diego, CA) (18, 19), where FAM indicates fluorescein and Q indicates dabcyl. The oligonucleotides were diluted in water to a final concentration of 100 μM and annealed in a 4:5 ratio of fluorescein- vs. dabcyl-labeled oligonucleotides. Release of the fluorescein-labeled oligonucleotide following cleavage at the abasic site by an AP endonuclease was achieved by thermal denaturation at 37 °C and followed in the kinetic mode with a Tecan Ultra 384 instrument using an excitation wavelength of 485 nm and emission of 535 nm. APE1 and APE1 C65/C93/C99 were assayed in 50 mM Tris 7.5, 125 mM NaCl, 1 mM $MgCl_2$, and 0.8% DMSO. Optimal concentrations of 0.04 nM APE1 and 0.06 nM APE1C65/C93/C99 were determined by varying the enzyme concentration at a fixed substrate concentration of 25 nM. The substrate was then varied from 0 to 75 nM to determine V_{max} and K_m values for this enzyme. DMSO was included in the assay in preparation for screening of small-molecule inhibitors dissolved in 0.8% DMSO and found not to affect the activity of the enzyme. Kinetic parameters were calculated from the average

of quadruplicate measurements for each substrate concentration using the Enzyme Kinetics module in SigmaPlot (SigmaPlot 11.2).

E3330 inhibition assay

E3330 was pre-incubated with 2 μL purified APE1 and substituted proteins reduced as described above in EMSA reaction buffer with total volume 16 μL for 30 min, and the EMSA assay was performed as previously described (12).

Cell growth and proliferation assays

Cell growth and proliferation was determined using the xCELLigence DP System (Roche Applied Science, Indianapolis IN), as previously described (12, 19-21). Briefly, Panc1 cells were transfected with a pcDNA empty vector, pcDNA-wtAPE1 or pcDNA-APE1 mutants by using lipofectamine TM 2000 in two 16-well plates of the xCELLigence DP System. Following 4 h transfection, fresh medium with fetal bovine serum (FBS) was added to the transfected cell cultures to yield a final concentration of 10% FBS. Cell growth was monitored continuously and recorded as a cell index every 30 min for 66 h. The cell index was normalized to the 1 h time point in the xCELLigence analysis. The assays were performed in duplicate and repeated at least three times in independent experiments.

Oxidation of APE1 and reaction with TRXC32

200 μL samples of 10 μM wild-type APE1 and APE1 C65/C93/C99 in 10 mM Tris pH 8.0 was treated with 1 mM H_2O_2 for 1, 5, or 15 mins. at room temperature. A fourth sample of wild-type APE1 was incubated under the same conditions for 30 min. at which time the sample was split into 2 separate samples. One sample of 10 μM APE1 was incubated for an additional 30 min (60 min. total) in 1 mM H_2O_2 and then quenched with NEM at a final concentration of 2 mM for 15 min prior to freezing at −80 °C. The second sample of 10 μM APE1 was incubated with 10 μM TRXC32 for 30 min. and then quenched with NEM, final concentration 2 mM, for 15 min prior to freezing at −80 °C. Two independent experiments were performed for the oxidation of APE1 with H_2O_2 and subsequent reaction with TRXC32; for both experiments, the same result was obtained.

LC-ESI-MS/MS Analysis of Protein Digests

10 μL of a 10 μM protein sample was diluted to 50 μL with 10 mM Tris-HCl (pH 8.0) buffer, and the diluted protein sample was digested using a protein:trypsin ratio of 50:1 at 37 °C for 16 h. The digestion reaction was quenched by adding 1 μL of concentrated acetic acid. Three independent replicates of the digestion experiment were performed. The digestion solution from each digestion replicate was then analyzed by LC-MS/MS whereby 5 μL of quenched digestion solution was loaded onto a Dionex Acclaim PepMap Nano trap column and desalted with 0.1% formic acid at 8 μL/min for 7 min. Peptides were then separated by using a silica capillary column with a PicoFrit tip (New Objective, Inc., Woburn, MA) by using a linear gradient supplied by a Dionex Ultimate 3000 (Dionex, Synnyvale, CA) and run at 260 nL/min from 20% to 55% acetonitrile, 0.1% formic acid, over 70 min. The silica capillary was custom packed with C18 reverse phase material (Magic, 0.075 mm ×150 mm, 5 μm, 120 Å, Michrom Bioresources, Inc., Auburn, CA). The flow was directed by a PicoView Nanospray Source (PV550, New Objective, Inc., Woburn, MA) into an LTQ FTICR mass spectrometer (Thermo-Scientific, San Jose, CA) with a spray voltage of 1.8-2.0 kV and a capillary voltage of 27 V. The LTQ FTICR was operated in standard data-dependent acquisition mode controlled by Xcalibur 2.0.7 software. Peptide mass spectra (*m*/*z* range 300-2000) were acquired at high mass resolving power (100,000 for ions of *m*/*z* 400). In the data-dependent mode, the six most abundant multiply charged ions with a minimum intensity of 1000 counts were subjected to collision induced dissociation

(CID) in the linear ion trap. Precursor activation in CID was performed with an isolation width (m/z) of 1, an activation time of 30 ms, and normalized collision energy of 35% of maximum. The LTQ FTICR was externally calibrated using a standard mixture of caffeine, MRFA, and Ultramark 1621. The mass calibration was checked and repeated before the LC-MS experiments to optimize the mass measurement accuracy.

Disulfide bonds search and analysis

The MS/MS *.raw data files were converted to *.mgf files with DTASuperCharge (V 2.0a6 from the open source proteomics platform MSQuant, version 2.0a81)(22) and then submitted to MassMatrix, an custom search engine developed by Xu et al.(23-25). The enzyme was set to “trypsin”; the maximum number of missed cleavages was two; the peptide mass tolerance was 5 ppm, allowing for one ^{13}C peak; and the peptide charge was allowed to be +1, +2, or +3. The production mass tolerance was 0.8 Da. The variable modifications chosen were NEM modification of cysteine and oxidation of methionine. The production (MS/MS) spectra of all of the identified disulfide contained peptide ions from the MassMatrix search were further manually inspected, and only those whose spectra were consistent with the assigned peptide were used.

Preparation and purification of APE1C99-TRXC32 disulfide-bonded species

For this experiment, an N-terminally truncated version of APE1 including only Cys 99 with all other Cys residues mutated to Ala (40APE1 C99) was used. As described above for other APE1 mutants, site-directed mutagenesis with the Stratagene Quikchange kit was used to introduce mutations, which were confirmed by DNA sequencing. The protein was expressed and purified as previously described (12, 26). A sample of 200 μL of 100 μM 40APE1 C99,1 mM diamide,10 mM Tris-Cl, pH 8.0 and 0.1 M NaCl was incubated at room temperature for 30 min, and then was dialyzed against 10 mM Tris-Cl, pH 8.0, 0.1 M NaCl at 4 °C overnight. 200 μL of 2 mM TRXC32,1 mM DTT, 10 mM Tris-Cl, pH 8.0 and 0.1 M NaCl was incubated at room temperature for 30 min, and then was dialyzed against 10 mM Tris-Cl, pH 8.0, 0.1 M NaCl at 4 °C overnight. The TRXC32 sample was diluted to 1 mL with 10 mM Tris-Cl, pH 8.0 and 0.1 M NaCl, incubated with 0.5 mL Ni-NTA agarose beads at 4 °C for 1 h by nutating, washed thoroughly with 10 mM Tris-Cl, pH 8.0, 0.1 M NaCl, 20 mM imidazole, and then incubated with the 40APE1 C99 sample overnight at 4 °C by nutating. The Ni-NTA beads with TRXC32 and 40APE1 C99 samples were washed thoroughly with 10 mM Tris-Cl, pH 8.0, 0.1 M NaCl, 20 mM imidazole, followed by elution with 10 mM Tris-Cl, pH8.0, 0.1 M NaCl, and 250 mM imidazole. The result was analyzed on a non-reducing SDS PAGE gel. The 40APE1 C99-TRXC32 disulfide-bonded species was further purified by size exclusion chromatography using a Superdex 200 column run in 50 mM Tris pH 8.0, 0.5 M NaCl.

Results

Identification of redox active Cys residues in APE1

We and others demonstrated that Cys 65 is required for the redox activity of APE1, and that Cys 93 also participates in the redox activity(12, 27). To determine whether other Cys residues might be involved in the redox activity of APE1, we analyzed double Cys mutants including C93A and substitutions of the other Cys residues, excluding Cys 65. C65A APE1 is redox inactive; thus, any additional involvement of Cys residues in the redox activity would be masked in the context of this mutant. The selection of double mutants including C93A was based on the finding that the redox activity of the C93A substituted APE1, as assessed by redox EMSA analysis and cell-based transactivation assays, is approximately 50% that of the wild-type protein, whereas individual substitution of Cys residues 99, 138, 208, 296, or 310 had no significant effect on the redox activity (11). Therefore, C99, C138,

C208, C296, and C310 were individually substituted with Ala along with C93 to create double mutants. The substituted APE1 proteins were tested for their ability to reduce c-Jun/c-Fos, which then binds DNA, resulting in a shifted band in a redox EMSA assay. Of the double Cys mutants, all but C93A/C99A retained approximately 50-60% redox activity. As the C93A mutant alone retains approximately 50% activity, the additional substitutions did not reduce further the redox activity. However, the redox activity of the C93A/C99A enzyme was reduced to ~ 10% of wild-type activity in this analysis, indicating a significant loss of redox activity (Figure 1A and 1B).

To confirm the results of *in vitro* EMSA redox assays, the double mutant C93A/C99A was compared to a subset of single mutants in a cell-based transactivation assay in which luciferase activity is dependent upon reduction and binding of NF-κB, a known APE1 redox target, to its target DNA binding sequence (12). In this assay, as shown in Figure 1C, the C93A mutant has diminished activity as compared to wt APE1 while C99A, C138A, and C208A mutants have close to wild-type activity. The double mutant C93A/C99A was redox-inactive in this assay with loss of activity comparable to that of the C65A mutant. The triple mutant C93A/C99A/C138A and the quadruple mutant C93/C99A/C138A/C208A were also redox-inactive in the transactivation assay. Thus, these results suggest that three Cys residues are involved in the redox activity of APE1, C65, C93, and C99.

Three Cys residues are necessary and sufficient for redox activity in APE1

To determine whether C65, C93, and C99 are sufficient for redox activity in APE1, we constructed and expressed APE1 that has only these Cys residues (APE1 C65/C93/C99). All other Cys residues were substituted with Ala (i.e., C138A, C208A, C296A, and C310A). APE1 C65/C93/C99 was then tested for redox activity in the redox EMSA and cell-based transactivation assays and found to retain wild-type redox activity, as shown in Figures 2 and 3. We next analyzed single Cys mutants introduced within APE1 C65/C93/C99 to assess the contributions of each Cys residue to the redox activity of APE1. To do this, we introduced substitutions resulting in APE1 that has only two Cys residues, C65/C93, C65/C99, or C93/C99; for these proteins, C99, C93, or C65 were substituted with Ala, respectively. The mutant APE1 proteins were then tested for redox activity in the EMSA redox and cell-based transactivation assays (Figures 2 and 3). Of these, C65/C93 and C65/C99 both showed decreases of ~50% in redox activity as compared to wild-type or APE1 C65/C93/C99 activity, whereas APE1 C93/C99 was redox-inactive. The activity measured for APE1 C65/C99 is consistent with the results we obtained previously for the C93A mutant (12). Further, the decrease in redox activity observed for APE1 C65/C93 confirms a role in the redox activity for Cys 99, as suggested by the double mutant experiments discussed above. Finally, we assessed APE1 including a single Cys residue, APE1 C65, for redox activity. In both the redox EMSA and transactivation assays, APE1 C65 was redox inactive, equivalent to the APE1 C93/C99 enzyme. Thus, a single Cys residue is not sufficient to confer redox activity. These results provide more evidence that C65, C93, and C99 are all involved in the redox activity of APE1.

It is also of interest to determine whether substitution of C138, C208, C296, and C310 in the APE1 C65/C93/C99 enzyme affects the endonuclease activity of the enzyme. In a steady state kinetic analysis, similar K_m values of 9.3 nM and 17.9 nM and V_{max} values of 123,000 and 110,000 (RFU/μg/s) were determined for the wild-type and C65/C93/C99 enzymes, respectively (Figure 4). Thus, the C65/C93/C99 enzyme retains near wild-type endonuclease activity, suggesting that the Cys residues that were substituted with Ala do not contribute significantly to the endonuclease activity of APE1. Both C65/C93 and C65/C99 enzymes also retain wild-type endonuclease activity (28). To test whether the substitutions affect the protein structure, we measured the CD spectra and found they are similar (Figure 1 of

Supporting Information) to that of the wild-type protein, suggesting that they retain a native-like state.

Effect of the redox inhibitor E3330 on APE1 and mutants

To assess further the redox properties of APE1 C65/C93/C99 and its mutants, we examined the inhibition of redox activity by (*E*)-3-(2-(5,6-dimethoxy-3-methyl-1,4-benzoquinonyl))-2-nonyl propenoic acid (E3330). E3330 was previously shown to inhibit specifically the redox function of APE1(11, 12, 17, 26). Using E3330 in EMSA experiments, as shown in Figure 5, we determined that E3330 blocks the redox activity of APE1 C65/C93/C99, APE1 C65/C93 and APE1 C65/C99, as well as wt-APE1 in a dose-dependent manner; the IC50's are18.8 μM, 21.7 μM, 18.9 μM and 17.4 μM, respectively. The ability of E3330 to inhibit the redox activity of APE1 C65/C93/C99 as well as redox-active APE1 C65/C93 and C65/C99 mutants at similar IC50's to that of wild-type APE1 suggests that all of these enzymes reduce AP-1 by a similar mechanism.

Effect of APE1 Cys mutants on cell proliferation in Panc1 cells

To determine the effect of APE1's redox activity on stimulation of cell proliferation, we compared the growth of cells transfected with pcDNA-wtAPE1, pcDNA-APE1 Cys mutants, or pcDNA (Figure 6). APE1 mutants include those analyzed for redox activity. Redox-inactive mutants include C65A, C65 only, or C93/C99 only, redox-impaired mutants C65/C93 or C65/C99 only, and the redox-active mutant C65/C93/C99. Cell growth was monitored by using the xCELLigence DP system (Figure 6), for which data were obtained every 30 min for 66 h. The redox-active mutant APE1C65/C93/C99 stimulated cell growth that was comparable to that of the wtAPE1, whereas the redox-impaired mutants did not stimulate cell growth and, in fact, had slower cell growth comparable to or lower than that observed for the control pcDNA vector. The redox inactive mutants, C65A and C93/C99 only, showed slower cell growth as compared to the control pcDNA vector. These results confirm an important role for the redox activity of APE1 in stimulating growth of cells, in this case Panc1 cells.

Disulfide bond formation in APE1

Thiol-mediated redox reactions necessarily involve the formation of disulfide bonds in the redox factor, which is oxidized in the process of reducing another protein. Oxidized APE1 is then reduced by another cellular redox factor such as thioredoxin (29). Here, we report LC-MS/MS analysis of trypsin-digested samples to identify both disulfide bonds formed in APE1 following oxidation with H_2O_2 and mixed disulfide bonds formed between oxidized APE1 and thioredoxin. The use of H_2O_2 serves to induce disulfide bond formation (30-33) through oxidation of Cys residues to sulfenic acid, making them susceptible to nucleophilic attack by a thiolate within the protein; the disulfide-bonded state of APE1 is recognized and reduced by thioredoxin. To trap mixed disulfide bonds involving thioredoxin and APE1, an engineered thioredoxin containing only the nucleophilic Cys 32(34) (TRXC32) was used. Of the five Cys residues in thioredoxin, all but Cys 32 were substituted with either Ser or Ala (see Experimental Procedures).

Both wild-type APE1 and APE1 C65/C93/C99 were incubated with 1 mM H_2O_2 for 1, 5, 15, or 60 min prior to quenching with the irreversible Cys-modifying reagent *N*-ethylmaleimide (NEM), which prevents disulfide bond scrambling during further sample manipulation. APE1 contains seven Cys residues; thus, there are 21 possible unique disulfide bonds involving two different Cys residues. Of the seven cysteines present in APE1, only C99 and C138 are solvent accessible, with C138 being the most accessible. Disulfide bonds were identified from three independent digests of each sample and analyzed by LC-MS/MS (see Experimental Procedures). Only the disulfide-bonded peptides that were

observed in all three replicates for the different time points and at significant levels are shown in Table 1. The disulfide-bonded peptides were identified by using Mass Matrix, a proteomics engine (see Experimental Procedures) that searches the LC/MS-MS data and confirmed by manual searching of all cysteine-containing peptides. We are only able to detect the disulfide-bonded peptides and not quantify them because they all respond differently to ESI and their response factors are unknown.

No disulfide bonds were observed for the 1 min. sample. After 5 min., a single disulfide bond, C65-C138, was observed in the wild-type APE1 sample. Incubation for 15 min. resulted in the formation of 4 disulfide bonds C65-C138, C65-C99, C93-C138, and C138-C208, and after 60 min. 10 disulfide bonds were observed (Table 1). In the APE1 C65/C93/C99 sample, no disulfide bonds were observed in 1 and 5 min. samples; a single disulfide bond C65-C99 was observed after 15 min. All possible disulfide bonds were observed in the 60 min. sample, C65-C93, C93-C99, and C65-C99. Thus, for each sample, the first disulfide bond formed between C65 and a solvent accessible cysteine, C138, in the case of the wild-type protein and C99 in the APE1 C65/C93/C99 protein. Subsequent disulfide bonds formed at later time points in each sample likely involve resolution of the first disulfide bond formed followed by further scrambling of disulfide bonds. Although we can determine which cysteines are involved in the disulfide bonds based on the LC-MS/MS results, we cannot determine whether the disulfide bonds are intermolecular or intramolecular. To assess the possibility of intermolecular disulfide bond formation, APE1 samples treated with H_2O_2 for 60 min were analyzed by non-reducing SDS-PAGE (Figure 7A), and high molecular weight bands (> 135 kDa) were observed consistent with the formation of intermolecular disulfide bonds leading to large complexes of APE1.

To determine whether a disulfide-bonded species of APE1 is recognized by thioredoxin, APE1 was incubated with 1 mM H_2O_2 for 30 min and then reacted with TRXC32 for an additional 30 min at room temperature. Following incubation with TRXC32, three new bands were observed on the non-reducing SDS gel, corresponding to ~ 30 kDa, ~60 kDa, and >135 kDa (Figure 7A). The ~30 kDa band corresponds to a dimeric species of disulfide-bonded TRX32C. The ~60 kDa and > 135 kDa bands likely correspond to mixed disulfide-bonded species including both APE1 and TRXC32; this conclusion is based on a comparison of the APE1 sample treated with H_2O_2 and control APE1 and TRXC32 samples (Figure 7). We hypothesize that the mixed disulfide-bonded species arise through reaction of TRXC32 with the high molecular weight species of APE1 observed in the oxidized APE1 sample as this band appears to decrease in intensity as compared to that corresponding to monomeric APE1, which appears to remain constant in a comparison of the oxidized APE1 vs. oxidized APE1 treated with TRXC32 (Figure 7A).

Mixed disulfide-bond formation was analyzed for the H_2O_2-oxidized APE1 reacted with TRXC32. The same ten disulfide bonds were observed for APE1 in this reaction as for APE1 treated only with H_2O_2 for 60 min. One mixed disulfide bond was found to form between C99 of APE1 and TRXC32. Formation of a disulfide bond between residues C99 of APE1 and C32 of TRX could result from nucleophilic attack of TRXC32 on an existing disulfide bond involving C99 in APE1, attack of TRXC32 on a sulfenic acid oxidized form of C99, or attack of C99 on an intermolecular disulfide-bonded TRXC32. As shown in Figure 7A, all of the TRXC32 is in an oxidized form for the sample reacted with oxidized APE1; there was no detectable band for reduced TRXC32.To characterize further the APE1-TRXC32 disulfide-bonded complex, we prepared an N-terminally truncated APE1 containing a single Cys residue (40APE1 C99) to ensure formation of a homogeneous disulfide-bonded sample. We previously showed that the N-terminally truncated APE1 retains near wild-type redox activity(11).The complex was prepared by treating 40APE1 C99 with diazenedicarboxylic acid *bis*[*N*,*N*-dimethylamide] (diamide), a thiol oxidizing

agent used to induce disulfide bond formation. The oxidized 40APE1 C99 was then reacted with reduced TRXC32. Ni-NTA affinity purification of the complex through use of the hexa-His tag on TRXC32 resulted in samples containing the mixed disulfide product, reduced 40APE1 C99, and reduced TRXC32. In further characterization by size exclusion chromatography, the mixed disulfide-bonded 40APE1 C99-TRXC32 species (~ 55 kDa band on a non-reducing SDS polyacrylamide gel, equivalent to the ~60 kDa product observed for the full-length APE1-TRXC32 sample) eluted from the column close to the void volume along with the dimeric disulfide-bonded 40APE1 C99 species. The estimated molecular weight for these disulfide-bonded species is greater than 700 kDa suggesting that these disulfide-bonded species form very large complexes in solution (Figure 7B). 40APE1 C99 and TRXC32 that coeluted with the mixed disulfide-bonded species in the Ni-NTA affinity purification eluted separately on the size exclusion column with apparent molecular weights of ~ 37 kDa and ~16 kDa, closely matching their calculated molecular weights of 32 and 14 kDa, respectively.

Discussion

Although APE1 has long been recognized as a redox factor, a detailed mechanism for APE1's oxidation and reduction had not yet been reported. In this study, we first identified three cysteine residues (C65, C93, and C99) as necessary and sufficient for APE1's redox activity. The involvement of all three Cys residues was confirmed through further substitution resulting in APE1 enzymes containing only C65/C93, C65/C99, and C93/C99; the first two showed a decrease of ~50% in redox activity whereas the latter was redox-inactive (Figure 3). In the context of the wild-type APE1 protein, substitution of Cys 99 with Ala does not decrease the redox activity of the protein, whereas for the C65/C93 APE1 protein, a significant loss in redox activity was observed (Figure 1C). These results suggest that other Cys residues within APE1 may partially compensate for the loss of Cys 99 in the C99A mutant. In contrast to thioredoxin, for which two Cys residues, the nucleophilic Cys 32 and resolving Cys 35 are required for redox activity (34), the involvement of three Cys residues in APE1's redox activity indicates a more complex redox mechanism.

We next analyzed a time course of disulfide bond formation upon oxidation of APE1. A single disulfide bond, C65-C138, formed within 5 min. of exposure to H_2O_2 in wild-type APE1, and within 15 min. C65-C99 formed in APE1 C65/C93/C99. As disulfide bond formation involves nucleophilic attack of a thiolate on an oxidized cysteine (a cysteine involved in a disulfide bond or a sulfenic acid form of the residue), a probable explanation for the formation of the single disulfide bond observed in wild-type APE1 is that C138, the most solvent accessible cysteine, was oxidized to a sulfenic acid form and attacked by the thiolate form of C65. Lacking C138, the single disulfide bond formed in APE1 (C65/C93/C99) may involve a similar attack of C65 on an oxidized C99, also a solvent accessible cysteine (Figure 8). Subsequently, in the 15 min. time point, additional new disulfide bonds likely result from nucleophilic attack on the original disulfide bond by another thiolate within APE1. This reaction resolves the original disulfide bond and results in the formation of new disulfide bonds. For wild-type APE1, resolution of the initial disulfide bond may involve nucleophilic attack by either C93 or C208 resulting in C93-C138 and C138-C208 disulfide bonds releasing C65 as a thiolate to react with oxidized C99 forming C65-C99 (Figure 8). This cascade of disulfide bond formation is consistent with what is observed for the APE1 (C65/C93/C99) sample in which the first disulfide bond formed is C65-C99. By 60 min., ten disulfide bonds formed in the wild-type APE1 resulting from further resolution of disulfide bonds that were formed at 15 min. The ten disulfide bonds include the same four observed for the 15 min. time point. In APE1 C65/C93/C99, three disulfide bonds formed after 60 min. As the C65-C99 bond formed first, we propose a resolving role for C93 in this protein similar to that seen in the wild-type protein.

In a previous study, we reported disulfide bond formation in μ40 APE1, which lacks the N-terminal 40 amino acids, following treatment with E3330 for 1 hour at 37 °C. In both control and E3330 treated samples, we observed C65-C93, C65-C99, C93-C99, and C93-C138 disulfide bonds (26), a subset of the disulfide bonds observed in the present study for full-length APE1 treated with H_2O_2 at room temperature for one hour. For the E3330-treated sample, C65-C138 was also observed (26). The amount of each disulfide bond formed following treatment with E3330 was significantly increased as compared to the control sample based on relative quantitation of each disulfide-bond containing peptide. Thus, the results from our previous study suggest that E3330 acts in a similar manner to H_2O_2 in inducing disulfide bond formation in APE1 consistent with our proposal that E3330 reacts transiently with cysteine residues in APE1 making them susceptible to nucleophilic attack.

What we have proposed here is a cascade that is consistent with the formation of the observed disulfide bonds as well as the mutational data in which C65, C93, and C99 are required for redox activity. The cascade is predicated on the initial disulfide bond formed being susceptible to nucleophilic attack by thiolates in APE1. Within one hour of oxidation with H_2O_2, all of the cysteine residues in APE1 were observed in disulfide bonds except C310. Peptide coverage in the LC-MS/MS experiments was overall 80-89%, and all cysteine-containing peptides were observed. There are, of course, other possible mechanisms that could explain the formation of the observed disulfide bonds in APE1. We propose one possible scenario that is consistent with all of the data.

Oxidized APE1 treated with TRXC32 resulted in the formation of a single mixed disulfide bond involving C99 from APE1. Considering the SDS-PAGE analysis of the reaction products and the results from the oxidation studies on APE1, we suggest that the most probable reaction involves nucleophilic attack of TRXC32 on a disulfide bond in APE1 involving C99. Within 15 min., the only disulfide bond involving C99 that forms in APE1 is C65-C99; by 60 min., two additional disulfide bonds form, C99-C138 and C99-C208. In this model, thioredoxin would attack one of these disulfide bonds resulting in the mixed disulfide.

A non-reducing SDS-PAGE analysis of the reaction of APE1 with H_2O_2 suggests that upon oxidation, APE1 forms intermolecular disulfide-bonded species, and that these larger complexes most likely react with TRXC32, giving rise to two distinct mixed disulfide-bonded species, one of molecular weight ~ 60 kDa and the other > 135 kDa (Figure 7). In further characterization by size exclusion chromatography of the mixed disulfide-bonded species, we find that both disulfide-bonded Δ40APE1 C99- Δ40APE1 C99 and the mixed disulfide-bonded 40APE1 C99-TRXC32 species form a very large complex that elutes from a Superdex 200 column with an apparent molecular weight greater than 700 kDa. The apparent molecular weights of the mixed disulfide-bonded or dimeric disulfide-bonded APE1 were unaltered when run in salt concentrations as high as 0.5 M NaCl. 40APE1 C99 that is not disulfide-bonded to TRXC32 elutes from the Superdex 200 column with an apparent molecular weight of 37 kDa, close to its expected MW of 32 kDa, suggesting that it adopts a native conformation. TRXC32 also elutes with an apparent MW of 16 kDa close to its expected MW of 14 kDa.

To address the functional significance of the APE1's redox function in the cell, we examined the effect of expressing fully redox-active, redox-impaired, and redox-inactive mutants of APE1 on cell growth in Panc1 cells. In real time cell-growth assays, redox-active APE1 enhanced cell growth as compared to the control. Conversely, redox-impaired or inactive mutants showed either no enhancement or decreased cell growth (Figure 6) consistent with an important functional role for APE1's redox activity in cell growth.

Thus, the results of the time course analysis of disulfide bond formation in both APE1 and the mutational results are consistent with a role for C65 as the nucleophilic cysteine, while C93 and C99 likely play roles in resolving disulfide bonds that are formed in APE1 upon oxidation. As a buried residue, C65 is less susceptible to oxidation than the solvent accessible Cys residues C99 and C138. However, to serve as a nucleophile in the formation of a disulfide bond, it must become accessible. This can occur through local unfolding, which we characterized in a study of the interaction of E3330 with APE1 where we discovered that APE1 exists in both native and partially unfolded conformations (26). In the partially unfolded conformation of APE1, C65 would be accessible, consistent with the disulfide bonding results. It has also been reported that the region including residues 80-85 that buries C65 in the structure has higher than average B-factors consistent with greater mobility in this region of the structure (14) allowing accessibility to C65.

The redox-active Cys residues are clustered in one of the two beta sheets that make up the beta sandwich fold of the APE1 structure. C65 and C93 are located within adjacent strands in the middle of one of the beta sheets within APE1, albeit positioned on opposite sides of the sheet, while C99 is located within a connecting loop region (Figure 9). The distinct properties of APE1 involving three Cys residues, the potential involvement of intermolecular disulfide bonds, and the formation of a large complex upon mixed disulfide bond formation with thioredoxin distinguish APE1 from other redox factors and suggest a unique redox mechanism.

Supplementary Material

Refer to Web version on PubMed Central for supplementary material.

Acknowledgments

We thank Sarah Delaplane in the Georgiadis laboratory for technical assistance in the preparation of APE1 samples and kinetic analyses, Dr. Melissa Fishel for help in construction of the various APE1 Cys mutants, and Drs. Quyen Hoang, Wei Wang, and Jingling Liao for assistance with CD experiments.

†This work was supported by a grant from the National Institutes of Health, CA114571 to M.M.G., CA121168, CA114571, CA121168S1 and the Riley Children's Foundation to M.R.K., and a grant from the National Institutes of Health, NCRR (2P41RR000954), to M.L.G.

Abbreviations

APE1	apurinic/apyrimidinic endonuclease
Cys	cysteine
E3330	(*E*)-3-(2-(5,6-dimethoxy-3-methyl-1,4-benzoquinonyl))-2-nonyl propenoic acid
ESI-MS	electrospray ionization mass spectrometry
FBS	fetal bovine serum
NEM	N-ethyl maleimide
diamide	diazenedicarboxylic acid *bis*[*N*,*N*-dimethylamide]
PDB	phosphate buffered saline
SDS-PAGE	sodium dodecyl sulfate polyacrylamide gel electrophoresis.

References

1. Trachootham D, Lu W, Ogasawara MA, Nilsa RD, Huang P. Redox regulation of cell survival. Antioxid Redox Signal. 2008; 10:1343–1374. [PubMed: 18522489]
2. Luo M, He H, Kelley MR, Georgiadis MM. Redox regulation of DNA repair: implications for human health and cancer therapeutic development. Antioxid Redox Signal. 2010; 12:1247–1269. [PubMed: 19764832]
3. Xanthoudakis S, Curran T. Identification and characterization of Ref-1, a nuclear protein that facilitates AP-1 DNA-binding activity. EMBO J. 1992; 11:653–665. [PubMed: 1537340]
4. Abate C, Patel L, Rauscher FJ 3rd, Curran T. Redox regulation of fos and jun DNA-binding activity in vitro. Science. 1990; 249:1157–1161. [PubMed: 2118682]
5. Matthews JR, Wakasugi N, Virelizier JL, Yodoi J, Hay RT. Thioredoxin regulates the DNA binding activity of NF-kappa B by reduction of a disulphide bond involving cysteine 62. Nucleic Acids Res. 1992; 20:3821–3830. [PubMed: 1508666]
6. Toledano MB, Leonard WJ. Modulation of transcription factor NF-kappa B binding activity by oxidation-reduction in vitro. Proc Natl Acad Sci U S A. 1991; 88:4328–4332. [PubMed: 1903539]
7. Shimizu N, Sugimoto K, Tang J, Nishi T, Sato I, Hiramoto M, Aizawa S, Hatakeyama M, Ohba R, Hatori H, Yoshikawa T, Suzuki F, Oomori A, Tanaka H, Kawaguchi H, Watanabe H, Handa H. High-performance affinity beads for identifying drug receptors. Nat Biotechnol. 2000; 18:877–881. [PubMed: 10932159]
8. Ema M, Hirota K, Mimura J, Abe H, Yodoi J, Sogawa K, Poellinger L, Fujii-Kuriyama Y. Molecular mechanisms of transcription activation by HLF and HIF1alpha in response to hypoxia: their stabilization and redox signal-induced interaction with CBP/p300. Embo J. 1999; 18:1905–1914. [PubMed: 10202154]
9. Ueno M, Masutani H, Arai RJ, Yamauchi A, Hirota K, Sakai T, Inamoto T, Yamaoka Y, Yodoi J, Nikaido T. Thioredoxin-dependent redox regulation of p53-mediated p21 activation. J Biol Chem. 1999; 274:35809–35815. [PubMed: 10585464]
10. Walker LJ, Robson CN, Black E, Gillespie D, Hickson ID. Identification of residues in the human DNA repair enzyme HAP1 (Ref-1) that are essential for redox regulation of Jun DNA binding. Mol Cell Biol. 1993; 13:5370–5376. [PubMed: 8355688]
11. Georgiadis MM, Luo M, Gaur RK, Delaplane S, Li X, Kelley MR. Evolution of the redox function in mammalian apurinic/apyrimidinic endonuclease. Mutat Res. 2008; 643:54–63. [PubMed: 18579163]
12. Luo M, Delaplane S, Jiang A, Reed A, He Y, Fishel M, Nyland RL 2nd, Borch RF, Qiao X, Georgiadis MM, Kelley MR. Role of the multifunctional DNA repair and redox signaling protein Ape1/Ref-1 in cancer and endothelial cells: small-molecule inhibition of the redox function of Ape1. Antioxid Redox Signal. 2008; 10:1853–1867. [PubMed: 18627350]
13. Gorman MA, Morera S, Rothwell DG, La Fortelle E, Mol CD, Tainer JA, Hickson ID, Freemont PS. The crystal structure of the human DNA repair endonuclease HAP1 suggests the recognition of extra-helical deoxyribose at DNA abasic sites. EMBO J. 1997; 16:6548–6558. [PubMed: 9351835]
14. Beernink PT, Segelke BW, Hadi MZ, Erzberger JP, Wilson DM 3rd, Rupp B. Two divalent metal ions in the active site of a new crystal form of human apurinic/apyrimidinic endonuclease, Ape1: implications for the catalytic mechanism. J Mol Biol. 2001; 307:1023–1034. [PubMed: 11286553]
15. Mol CD, Izumi T, Mitra S, Tainer JA. DNA-bound structures and mutants reveal abasic DNA binding by APE1 and DNA repair coordination [corrected]. Nature. 2000; 403:451–456. [PubMed: 10667800]
16. Kelley MR, Luo M, Reed A, Su D, Delaplane S, Borch RF, Nyland RL 2nd, Gross ML, Georgiadis MM. Functional analysis of novel analogues of E3330 that block the redox signaling activity of the multifunctional AP endonuclease/redox signaling enzyme APE1/Ref-1. Antioxid Redox Signal. 2011; 14:1387–1401. [PubMed: 20874257]
17. Nyland RL, Luo M, Kelley MR, Borch RF. Design and synthesis of novel quinone inhibitors targeted to the redox function of apurinic/apyrimidinic endonuclease 1/redox enhancing factor-1 (Ape1/ref-1). J Med Chem. 2010; 53:1200–1210. [PubMed: 20067291]

18. Madhusudan S, Smart F, Shrimpton P, Parsons JL, Gardiner L, Houlbrook S, Talbot DC, Hammonds T, Freemont PA, Sternberg MJ, Dianov GL, Hickson ID. Isolation of a small molecule inhibitor of DNA base excision repair. Nucleic Acids Res. 2005; 33:4711–4724. [PubMed: 16113242]
19. Bapat A, Glass LS, Luo M, Fishel ML, Long EC, Georgiadis MM, Kelley MR. Novel small-molecule inhibitor of apurinic/apyrimidinic endonuclease 1 blocks proliferation and reduces viability of glioblastoma cells. J Pharmacol Exp Ther. 2010; 334:988–998. [PubMed: 20504914]
20. Jiang Y, Zhou S, Sandusky GE, Kelley MR, Fishel ML. Reduced expression of DNA repair and redox signaling protein APE1/Ref-1 impairs human pancreatic cancer cell survival, proliferation, and cell cycle progression. Cancer Invest. 2010; 28:885–895. [PubMed: 20919954]
21. Fishel ML, He Y, Reed AM, Chin-Sinex H, Hutchins GD, Mendonca MS, Kelley MR. Knockdown of the DNA repair and redox signaling protein Ape1/Ref-1 blocks ovarian cancer cell and tumor growth. DNA Repair (Amst). 2008; 7:177–186. [PubMed: 17974506]
22. Mortensen P, Gouw JW, Olsen JV, Ong SE, Rigbolt KT, Bunkenborg J, Cox J, Foster LJ, Heck AJ, Blagoev B, Andersen JS, Mann M. MSQuant, an open source platform for mass spectrometry-based quantitative proteomics. J Proteome Res. 2010; 9:393–403. [PubMed: 19888749]
23. Xu H, Zhang L, Freitas MA. Identification and characterization of disulfide bonds in proteins and peptides from tandem MS data by use of the MassMatrix MS/MS search engine. J Proteome Res. 2008; 7:138–144. [PubMed: 18072732]
24. Xu H, Freitas MA. A mass accuracy sensitive probability based scoring algorithm for database searching of tandem mass spectrometry data. BMC Bioinformatics. 2007; 8:133. [PubMed: 17448237]
25. Xu H, Yang L, Freitas MA. A robust linear regression based algorithm for automated evaluation of peptide identifications from shotgun proteomics by use of reversed-phase liquid chromatography retention time. BMC Bioinformatics. 2008; 9:347. [PubMed: 18713471]
26. Su D, Delaplane S, Luo M, Rempel DL, Vu B, Kelley MR, Gross ML, Georgiadis MM. Interactions of Apurinic/Apyrimidinic Endonuclease with a Redox Inhibitor: Evidence for an Alternate Conformation of the Enzyme. Biochemistry. 2011; 50:82–92.
27. Walker LJ, Robson CN, Black E, Gillespie D, Hickson ID. Identification of residues in the human DNA repair enzyme HAP1 (Ref-1) that are essential for redox regulation of Jun DNA binding. Mol. Cell. Biol. 1993; 13:5370–5376. [PubMed: 8355688]
28. Kim Y-J, Kim D, Illuzzi JL, Delaplane S, Su D, Bemier M, Gross ML, Georgiadis MM, Wilson DMI. S-Glutathionylation of cysteine 99 in the APE1 prpotein impairs abasic endonuclease activity. J. Mol. Biol. 2011 in press.
29. Hirota K, Matsui M, Iwata S, Nishiyama A, Mori K, Yodoi J. AP-1 transcriptional activity is regulated by a direct association between thioredoxin and Ref-1. Proc Natl Acad Sci U S A. 1997; 94:3633–3638. [PubMed: 9108029]
30. Men L, Roginskaya M, Zou Y, Wang Y. Redox-dependent formation of disulfide bonds in human replication protein A. Rapid Commun Mass Spectrom. 2007; 21:2743–2749. [PubMed: 17659658]
31. Day AM, Veal EA. Hydrogen peroxide-sensitive cysteines in the Sty1 MAPK regulate the transcriptional response to oxidative stress. J Biol Chem. 2010; 285:7505–7516. [PubMed: 20061379]
32. Chen CY, Willard D, Rudolph J. Redox regulation of SH2- domain-containing protein tyrosine phosphatases by two backdoor cysteines. Biochemistry. 2009; 48:1399–1409. [PubMed: 19166311]
33. Lametsch R, Lonergan S, Huff-Lonergan E. Disulfide bond within mu-calpain active site inhibits activity and autolysis. Biochim Biophys Acta. 2008; 1784:1215–1221. [PubMed: 18501725]
34. Holmgren A. Thioredoxin structure and mechanism: conformational changes on oxidation of the active-site sulfhydryls to a disulfide. Structure. 1995; 3:239–243. [PubMed: 7788289]

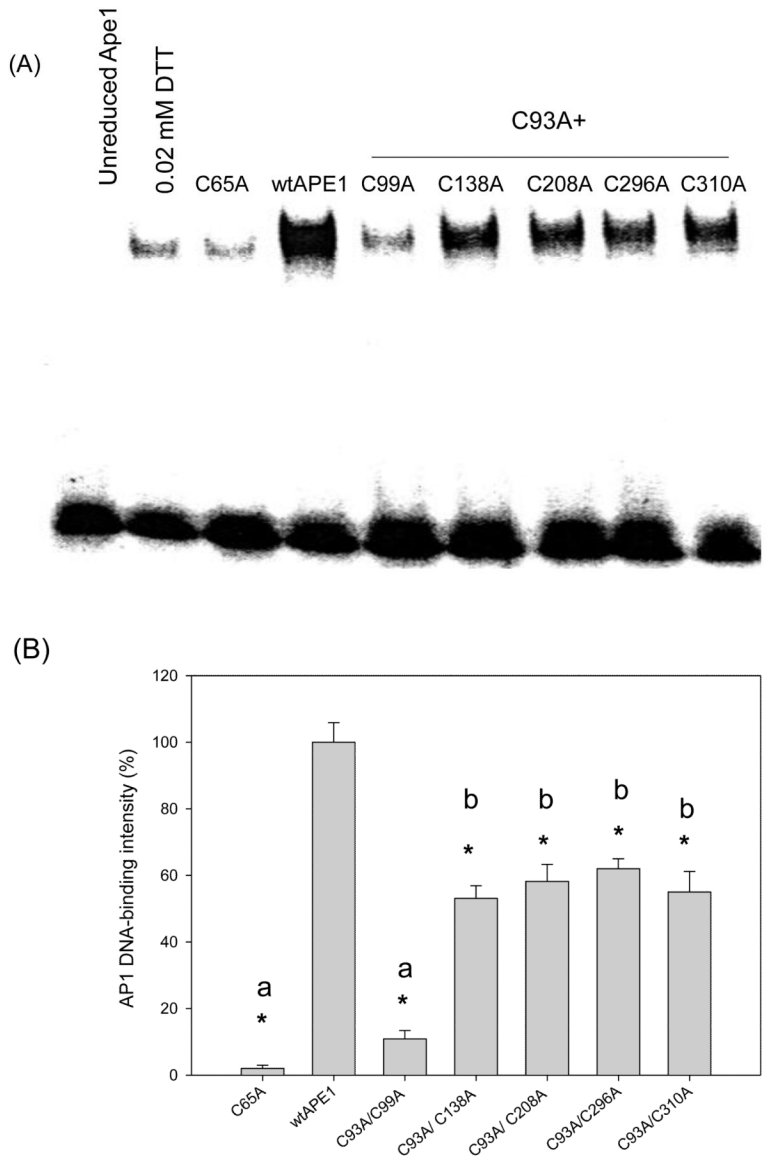

(C)

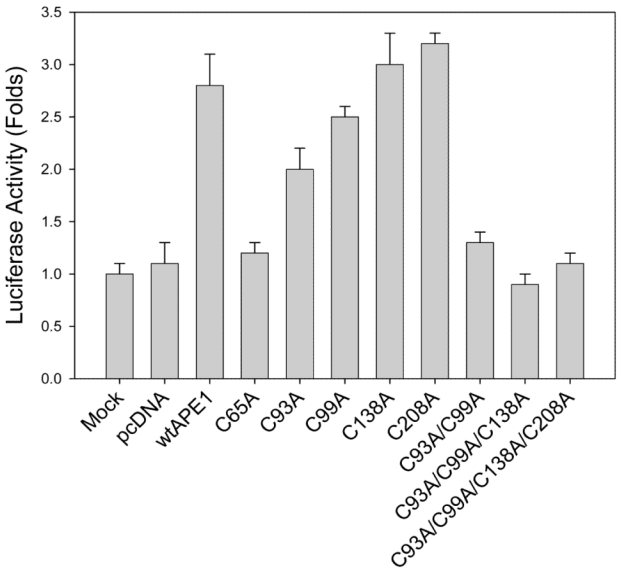

Figure 1. (A) EMSA redox assay for double Cys mutants including C93A

Reduced APE1 and its mutant proteins (reduced with 1mM DTT and then diluted to a final concentration of 0.02 mM DTT) or oxidized (unreduced) proteins were preincubated with purified truncated AP-1 protein (c-Jun/c-Fos) for 30 min and then the EMSA was performed as previously described (12, 16, 17). For the control lane, 0.02 mM DTT was used as a control for the DTT that is carried over from the protein reduction (Lane 2). Unreduced wtAPE1 protein (Lane1) and mutant proteins (data not shown) did not show redox activity. Reduced wt APE1 enhanced AP1 DNA-binding (Lane 4), whereas reduced C65A APE1 and double Cys mutant C93A/C99A APE1 did not (Lane 3, 5). And all other double Cys mutants including C93A retain 50-60% redox activity (Lane 6-9). **(B)** Quantization of the results of the experiments shown in A, above. Data are means ± standard error from three independent experiments and Student's t-tests were performed. The symbol * indicates a significant difference at $p < 0.05$ level compared with wt APE1 whereas "a" and "b" indicate there is no significant difference between the samples labeled "a" and among the samples labeled "b", respectively. **(C)** Transactivation assay results comparing C93A/ C99A to other mutants. Transactivation assays were performed as described in the Experimental Procedures and as previously published (12). All of the transfection experiments were performed in triplicate and repeated at least three times in independent experiments. Data are means ± standard derivation from one representative experiment. The C93A mutant has reduced activity as compared to wt APE1 whereas C99A, C138A, and C208A mutants have close to wild-type activity. The double mutant C93A/C99A was redox-inactive with activity comparable to that of the C65A mutant. No further reduction in activity was observed for the triple mutant C93A/C99A/C138A or quadruple mutant C93/C99A/C138A/C208A.

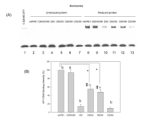

Figure 2. EMSA redox activity for APE1 including C65, C93, and C99 and mutants

(A) EMSA was performed as described in the Experimental Procedures. DTT (0.02 mM) was the control for DTT carry-over (Lane 1). Oxidized proteins (Lane 2-7) did not enhance AP-1-DNA binding. Reduced APE1 C65/ C93/ C99 and wt APE1 (Lane 8 and 9) APE1 C65 (Lane 10 and 13) did not, whereas APE1 C65/C93, and APE1 C65/C99 (Lane 11-12) demonstrated a reduced, but intermediate binding pattern. **(B)** Quantization of the EMSA results. Data are means ± standard error from three independent experiments, and Student's t-tests were performed. The symbols * and ‡ indicate a significant difference at $p < 0.05$ level compared with wt APE1 and APE1 C65, respectively, whereas "a", "b", and "c" indicate there is no significant difference ($p > 0.05$) between samples labeled "a", between the samples labeled "b", and between the samples labeled "c", respectively.

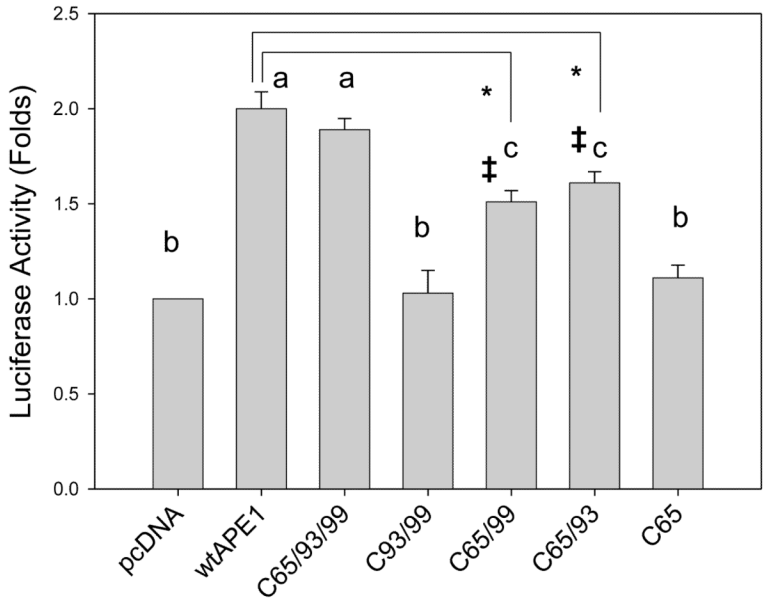

Figure 3. Cell-based transactivation data for wt APE1 and Cys restricted mutants

Skov-3X cells containing the NF-κB-Luciferase reporter construct were transfected with plasmid pcDNA-wtAPE1 or the mutant APE1 (pcDNA-C65/C93/C99, pcDNA-C93/C99, pcDNA-C65/C93, pcDNA-C65/C99, pcDNA-C65) and a *Renilla* luciferase control reporter vector pRL-CMV. After a 30 h transfection period, cells were lysed, and *Firefly* and *Renilla* luciferase activities were assayed using *Renilla* luciferase activity for normalization. All of the transfection experiments were performed in triplicates and repeated at least three times in independent experiments. Data are means ± standard error from three independent experiments, and Student's t-tests were performed. The symbols * and ‡ indicate significant difference at $p < 0.05$ level compared with wtAPE1 and the control sample (pcDNA), respectively, whereas "a", "b", and "c" indicate there is no significant difference ($p > 0.05$) between samples labeled "a", among the samples labeled "b", and between the samples labeled "c", respectively.

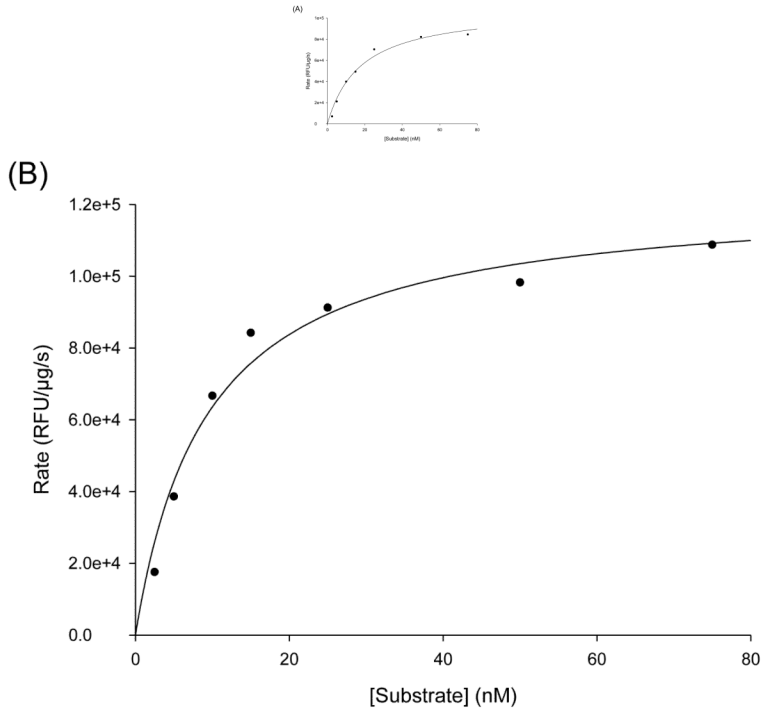

Figure 4. Enzymatic characterization of wild-type APE1 and the C65/C93/C99 APE1

A kinetic analysis of endonuclease activity was performed for wild-type APE1 (A) and APE1 C65/C93/C99 (B) using a fluorescence-based solution assay adapted from a previously reported assay (18). In this assay, the tetrahydrofuran-containing abasic site substrate mimic was varied in concentration from 0 to 75 nM with enzyme concentrations of 0.04 or 0.06 nM, respectively, for wild-type APE1 and APE1 C65/C93/C99. The maximal velocity and K_m values were calculated by using the Enzyme Kinetics module in SigmaPlot (SigmaPlot 11.2).

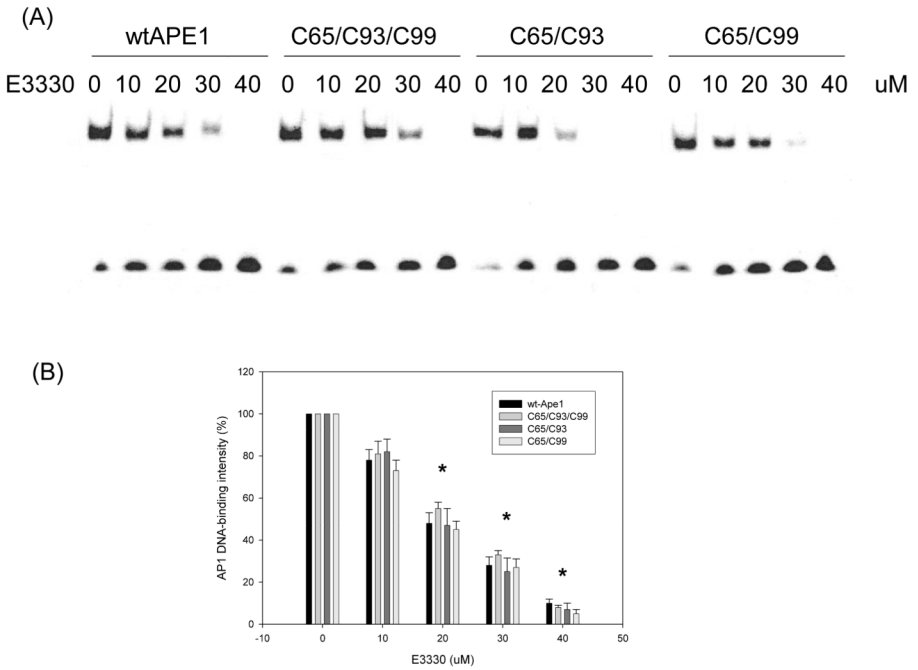

Figure 5. Inhibition of APE1 and minimally containing Cys mutants as compared to wt APE1 by the small molecule APE1 redox inhibitor E3330

(A) An increasing amount of E3330 was preincubated with 2 μL purified APE1 or its mutant proteins (APE1 C65/ C93/ C99, APE1 C65/C93, and APE1 C65/C99) (reduced with 1.0 mM DTT and then diluted to 0.006 mM with 0.02 mM DTT in PBS) in EMSA reaction buffer with a total volume 16 μL for 30 min and then the EMSA assay was performed. E3330 inhibited AP-1 DNA-binding enhanced by APE1 C65/C93/C99, APE1 C65/C93, APE1 C65/C99 and wt APE1 in a dose-dependent manner. **(B)** Quantization of the results of the experiments above. The redox activity of APE1 C65/C93/C99, APE1 C65/C93, APE1 C65/C99 and wt APE1 was inhibited by E3330 in a dose-dependent manner with 50% inhibition values of 18.8 μM, 21.7 μM 18.9uM and 17.4 μM, respectively. Data are means ± standard error from three independent experiments, and Student's t-tests were performed. The symbol * indicates the significant difference at $p < 0.01$ level compared with E3330-untreated sample. There is no significant difference ($p > 0.05$) comparing the IC50s of E3330 and the inhibition percentages at each dose of E3330 in APE1 C65/ C93/ C99, APE1 C65/ C93, and APE1 C65/C99 to those in wt APE1.

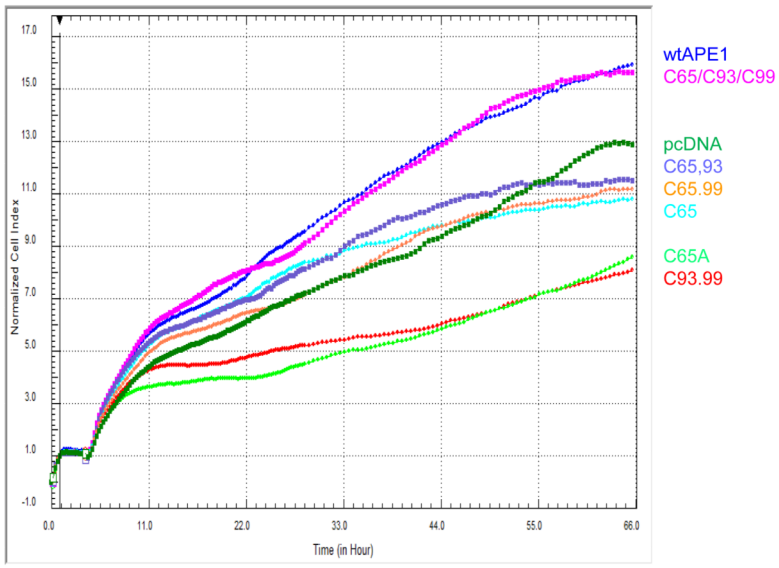

Figure 6. Effect of APE1 and its redox mutants on cell proliferation in Panc1 cells

Panc1 cells were transfected with a control pcDNA empty vector plasmid, pcDNA-wtAPE1 or the pcDNA-APE1 mutants using lipofectamine TM 2000 and analyzed by using the xCELLigence DP System, which measures cell growth in real time. After transfection (4 h), fresh medium with FBS was added. Data were obtained every 30 min for 66 h. Data from one representative experiment are shown. APE1 C65/93/99 stimulated cell growth and proliferation as did wt APE1, similar to what was observed by using an MTT analysis (data not shown). None of the other mutants stimulated growth; some displayed growth levels that were below that observed for the vector control.

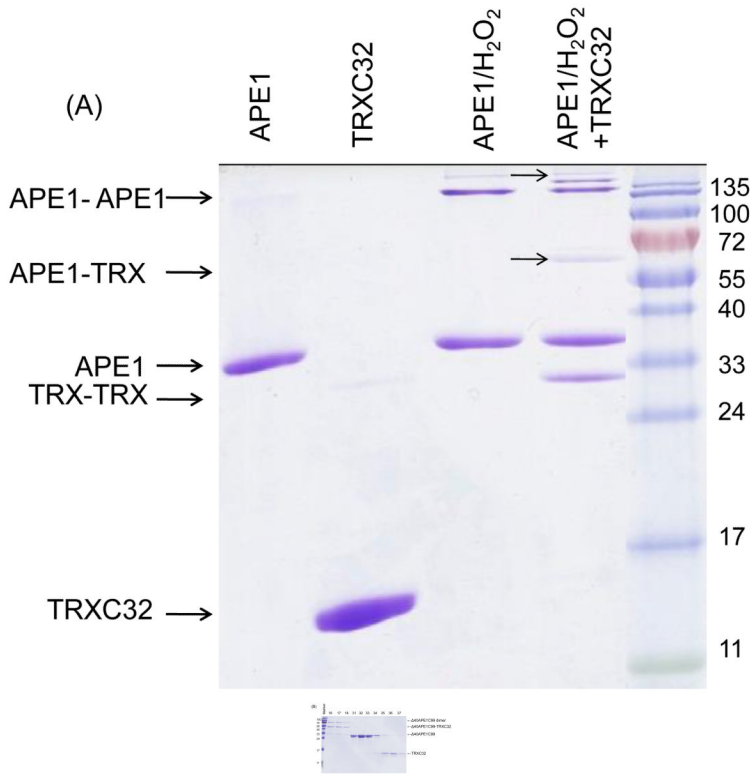

Figure 7. Non-reducing SDS-PAGE analysis of oxidized APE1 +/− TRXC32 (A) and purified disulfide-bonded APE1/TRX samples (B)

APE1 was oxidized by using H_2O_2 and then reacted with thioredoxin including a single Cys, the nucleophilic Cys 32 (TRXC32). Shown in (A) are control samples of APE1 and TRXC32 that were not reacted with H_2O_2, oxidized APE1, and oxidized APE1 reacted with TRXC32. APE1 appears to form intermolecular disulfide bonds leading to a product that runs on the gel with an approximate molecular weight greater than 135 kDa. Reaction with TRXC32 results in the appearance of two new bands (indicated by arrows) corresponding to mixed disulfide-bonded species that run at approximately 60 kDa and greater than 135 kDa. Shown in (B) are the fractions collected from the size exclusion gel chromatographic analysis of the Ni-NTA purified 40APE1 C99-TRXC32 disulfide-bonded complex. Fraction numbers are shown at the top of each lane. The void volume for the column, determined by using blue dextran 2000, is 8.0 ml, corresponding to fraction 16. The largest standard protein, thyroglobulin, with a molecular weight of 669 kDa elutes at a volume of 8.95 ml, corresponding to fraction 18. Thus, the apparent molecular weight of the 40APE1C99-TRXC32 complex is greater than 700 kDa based on this calibration. Molecular weight standards for the non-reducing SDS PAGE analysis are shown in the left most lane with sizes labeled. The mixed disulfide-bonded species runs on the SDS gel with an apparent molecular weight of ~ 55 kDa.

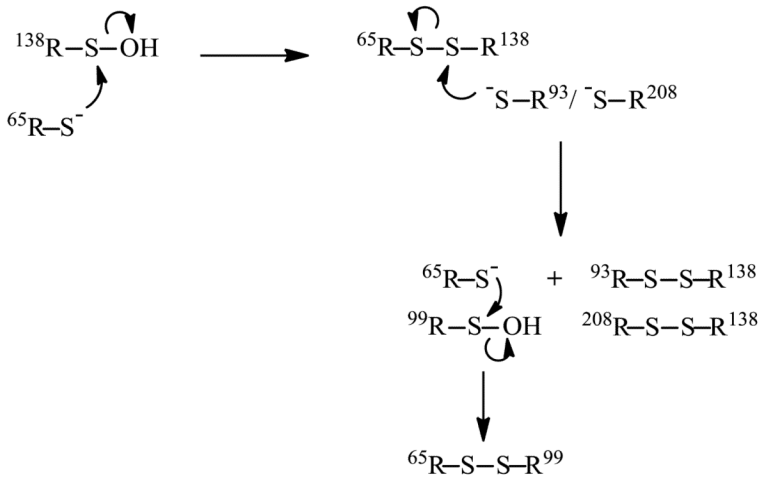

Figure 8. Schematic of a possible mechanism for the formation of disulfide bonds in APE1 is shown

Treatment of APE1 with hydrogen peroxide resulted in the formation of a single disulfide bond within 5 min. for wild-type APE1 between C65 and C138. Resolution of this disulfide bond through nucleophilic attack by either C93 or C208 would result in two of the four disulfide bonds observed following 15 min. exposure to hydrogen peroxide. This reaction would liberate C65 as a thiolate, which could subsequently attack oxidized C99 and form the fourth disulfide bond that was observed.

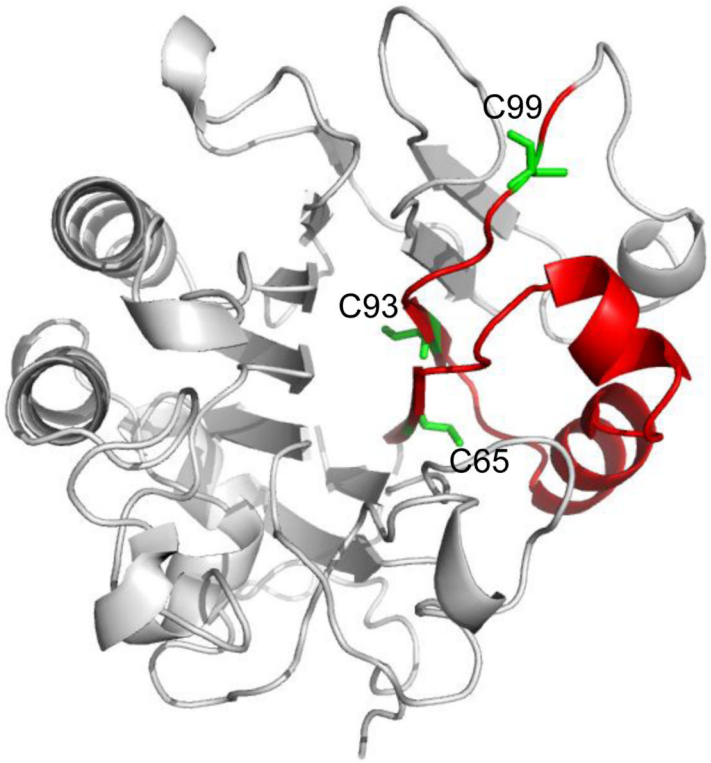

Figure 9. APE1 structure with redox active cysteines highlighted

A ribbon rendering of APE1 is shown in gray with C65, C93, and C99 shown in green stick renderings in a view showing the two beta sheets that comprise the beta sandwich fold. The two beta strands containing C65 and C93 along with the intervening helical element and the connecting loop region containing C99 are highlighted in red.

Table 1

Time course of disulfide bond formation for APE1 treated with H_2O_2

Time	Disulfide bond									
	65-138	**65-99**	**65-93**	**65-296**	**93-138**	**93-99**	**99-138**	**99-208**	**138-208**	**138-296**
1										
5	X									
15	X	X			X				X	
60	X	X	X	X	X	X	X	X	X	X